This article has been accepted for publication in IEEE Access. This is the author's version which has not been fully edited and content may change prior to final publication. Citation information: DOI 10.1109/ACCESS.2025.3626553

Impact of Spatial Correlation on Link Selection and Delay Performance in Multi-RIS Networks

Ahmed I. Abdulshakoor[1], (Student Member, IEEE), Najah Abu Ali[2], (Senior Member, IEEE), and Hossam S. Hassanein[3], (Fellow, IEEE)
[1]Department of Electrical and Computer Engineering, Queen's University, Kingston, ON, Canada (e-mail: ahmed.a@queensu.ca)
[2]College of Information Technology, United Arab Emirates University, Al-Ain, UAE (e-mail: najah@uaeu.ac.ae)
[3]School of Computing, Queen's University, Kingston, ON, Canada (e-mail: hossam@cs.queensu.ca)

ABSTRACT Reconfigurable Intelligent Surface (RIS) technology has emerged as a key enabler for enhancing the performance of wireless communication networks. We investigate the deployment of multiple RISs within a cellular coverage area to enable diverse link options. We analytically characterize the impact of spatial correlation among RIS elements and derive the signal-to-noise ratio (SNR) distribution for the direct link to the base station (BS) and the cascaded RIS-assisted link, under Nakagami-m fading. Building on this analysis, a comprehensive framework is developed to evaluate the average packet delay, addressing the gap in delay analysis under spatial correlation for multi-RIS systems. Moreover, we derive a closed-form condition to identify when the direct link outperforms RIS-assisted transmission, thus guiding link selection and RIS-user association based on delay performance. Numerical results highlight the substantial effect of spatial correlation on delay analysis and demonstrate that neglecting this factor can severely underestimate network performance by leading to suboptimal link selections. A high degree of correlation concentrates channel energy into a dominant eigenmode for single-user transmission, thereby enhancing the effective SNR. Furthermore, the results show that the proposed delay-based selection approach accurately evaluates feasible links with the aim of minimizing the average packet delay, achieving superior performance compared to benchmark methods.

INDEX TERMS Reconfigurable Intelligent Surface (RIS), multi-RIS network, RIS association, 5G and NextG networks, packet delay, spatial correlation.

I. INTRODUCTION

THE vision of sixth-generation (6G) wireless networks extends beyond conventional transceiver optimization to intelligent control of the propagation environment. In contrast to the conventional treatment of environmental objects and channel conditions as uncontrollable, 6G seeks to render them programmable to enhance coverage, capacity, and reliability. In this context, Reconfigurable Intelligent Surfaces (RISs) have emerged as a promising solution to enhance wireless network performance. An RIS is a planar surface composed of numerous low-cost passive elements that dynamically manipulate incident signals, creating a controllable propagation environment [1]. From an energy-efficiency perspective, wireless signals can be intelligently redirected and reflected without relying on power sources, radio frequency (RF) chains, or complex signal processing. This capability allows for the dense deployment of RISs across network infrastructures at low cost and without complicated management, leading to substantial improvements in overall quality of wireless communication services.

RIS offers a wide range of promising applications for future wireless networks. Particularly, in urban settings, where buildings obstruct wireless links and degrade quality of service (QoS), RISs improve coverage and reliability by intelligently reflecting signals to bypass obstacles, thereby enhancing overall connectivity and user experience. Furthermore, the geometry and lightweight design of RIS enables flexible deployment across both indoor and outdoor environments. It can be installed on building surfaces or carried by aerial platforms, offering considerable adaptability in network planning. By incorporating RIS into wireless systems, an intelligent radio environment can be established that adapts to varying user demands, supporting enhanced throughput, reduced power consumption, improved coverage, and secure communications [2], [3]. Consequently, RIS is expected to play a crucial role in the evolution of future wireless networks.

While extensive research has explored RIS-assisted wireless systems, most studies focus on single-RIS deployments [4]–[6], which offer limited coverage and channel control, especially in obstructed urban environments. These limitations can restrict the system's ability to meet stringent throughput and latency requirements. To address these challenges, some recent works have investigated multi-RIS architectures, where deploying multiple RISs enhances path diversity, improves link quality, and supports flexible transmission path selection to meet varying QoS demands. Consequently, dense

This article has been accepted for publication in IEEE Access. This is the author's version which has not been fully edited and content may change prior to final publication. Citation information: DOI 10.1109/ACCESS.2025.3626553

RIS deployment improves reliability, data throughput, and network scalability. In [7], multiple RISs were used to enhance millimeter-wave (mmWave) coverage when direct base station (BS)-user links were unavailable. A multi-RIS multi-BS downlink system was examined in [8], where RISs extended coverage into a blind spot, enabling users to receive signals from all RISs. The authors in [9] studied system energy efficiency by optimizing RISs on-off control through a matching algorithm. However, their model assumes that each active RIS serves all users without distinction, overlooking user-specific associations and thereby limiting resource efficiency. Other works [10]–[12] further explored multi-RIS setups. However, many studies consider that each user communicates with the BS through all available RISs, with reflection coefficients optimized individually, leading to inefficient resource utilization, high complexity, and scalability challenges.

Studying RIS-user association is crucial for efficient path selection, improved connectivity, and meeting diverse QoS demands, making it a key enabler for next-generation wireless networks. Various RIS association policies, including random selection, nearest RIS selection, and association with all RISs, were examined in [13], showing that their effectiveness depends on factors like the number of RIS elements and blockage density. In [14], users were assigned to the nearest RIS within a distance threshold, limiting the number of users per RIS. Additionally, a distance-based criterion was employed in [15], where each user is associated with the nearest RIS. The authors in [16] proposed an association method to balance passive beamforming gains from RISs, but it lacks flexibility and scalability for diverse link selections. In [17], an RIS-assisted cell-free network was investigated, in which multiple BSs cooperatively serve multiple users with the assistance of several distributed RISs. In this setup, each user was assumed to be assisted by a dedicated RIS while being connected to multiple BSs, with the objective of maximizing the minimum signal-to-interference-plus-noise ratio (SINR) among all users. In [18], the RIS selection problem was formulated as a one-to-one matching problem to achieve stable RIS-User matching and improve the system sum rate. The authors in [19] jointly considered the association between user-RIS, active beamforming design, and passive beamforming optimization in a multi-RIS-assisted wireless system. In [20], the authors formulated a joint optimization problem that involves active beamforming, passive beamforming, and RIS-user association, with the aim of maximizing the system sum-rate.

However, the majority of existing studies on RIS-user association overlook a critical factor– the spatial correlation among RIS elements. These works often assume uncorrelated channels, neglecting the correlation induced by the finite surface size and the small inter-element spacing of practical RISs, which is largely unavoidable [21]. Ignoring this correlation can lead to inaccurate performance evaluations and suboptimal system designs. Although some studies have considered RIS element correlation [21]–[26], they typically neglect its impact on user-RIS association and RIS selection in multi-RIS networks. Most of these works focus on single-RIS scenarios with limited scalability or design reflection coefficients for multi-RIS systems based on predefined RIS-user associations, thereby overlooking the interaction between correlation and RIS selection.

Moreover, these studies primarily optimize conventional performance metrics such as ergodic capacity, outage probability, or energy efficiency, while overlooking key QoS metrics like packet delay, which is crucial for next-generation networks.

This paper studies the deployment of multiple RISs within a cellular coverage area to provide a variety of link options. To the best of our knowledge, our work is the first to quantify the impact of spatial correlation among RIS elements on both packet delay and the link selection process, an aspect that has been largely overlooked in existing literature. The proposed link selection and RIS association method is guided by packet delay, a key metric for real-time applications and overall network performance. Our contributions are outlined as follows:

- We quantify the impact of spatial correlation among RIS elements on both individual channel performance and the overall cascaded RIS channel, providing new insights into how elements correlation influences link quality and network latency in multi-RIS systems.
- We present a comprehensive delay analysis for both the direct link to the BS and the RIS-assisted links, incorporating spatial correlation effects, and evaluate their impact on the link selection process.
- We utilize this analysis to derive a closed-form analytical condition, based on the signal-to-noise ratio (SNR) distribution, to determine scenarios where the direct BS link achieves superior performance over RIS-assisted paths in multi-RIS networks. This condition identifies the RIS options that are feasible for a user during the delay-based selection and association process.

We validate our approach through simulations and demonstrate its effectiveness in reducing packet delay compared to benchmark methods. Our results highlight the importance of incorporating spatial correlation among RIS elements, as neglecting this factor can lead to suboptimal link selection and, consequently, degrade the delay performance of the network.

The rest of this paper is organized as follows. In section II, the system model is described. Section III outlines packet delay analysis and introduces the link selection process. The performance evaluation and simulation results are provided in section IV, and finally, Section V concludes this paper.

II. SYSTEM MODEL

Consider a downlink wireless communication system enhanced by RIS technology, as depicted in Fig. 1. The system comprises a BS, K users, and I RISs. Each RIS r is equipped with N passive reflecting elements. We consider a slotted transmission, and assume a quasi-static flat-fading channel

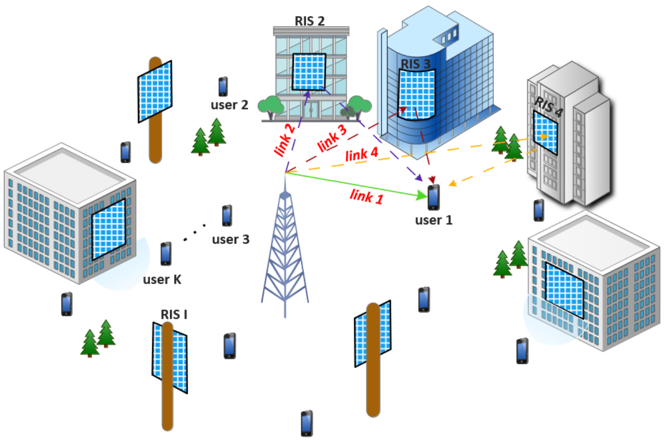

FIGURE 1. User association model in multi-RIS networks.

model, where all channels remain nearly constant during each channel coherence interval [27].

Let D_k, $h_r \triangleq [h_{r,1}, h_{r,2}, ..., h_{r,N}]^T \in \mathbb{C}^{N\times 1}$, and $g_{r,k} \triangleq [g^{(k)}_{r,1}, g^{(k)}_{r,2}, ..., g^{(k)}_{r,N}]^T \in \mathbb{C}^{N\times 1}$, denote the baseband equivalent channels of the direct link between BS and user k, from the BS to RIS r, and from the RIS r to the user k, respectively. The direct link's channel D_k to user k can be expressed as follows

$$D_k = d_k^{-\delta_k/2}\ \varkappa_k\ e^{-j\psi_k} \tag{1}$$

where d_k represents the distance between the BS and user k, δ_k is the corresponding path-loss exponent, $\varkappa_k$ is the channel amplitude modeled by a Nakagami-m distribution with shape parameter m_{d_k} and scale parameter Ω_{d_k}, and ψ_k is the channel's phase. Nakagami-m distribution provides versatility in modeling different fading conditions. Thus, the amplitude $|D_k|$ is a scaled Nakagami-m random variable (RV) with mean and variance given by [28]

$$\begin{aligned} \mu_k &= d_k^{-\delta_k/2}\ \frac{\Gamma(m_{d_k}+1/2)}{\Gamma(m_{d_k})}\ (\frac{\Omega_{d_k}}{m_{d_k}})^{1/2} \\ \sigma_k^2 &= d_k^{-\delta_k}\ \Omega_{d_k}\ \left(1 - \frac{1}{m_{d_k}}(\frac{\Gamma(m_{d_k}+1/2)}{\Gamma(m_{d_k})})^2\right) \end{aligned} \tag{2}$$

where $\Gamma(.)$ is the gamma function.

For the RIS-assisted link, the cascaded channel between the BS and user k via RIS r is denoted by $H_{r,k}$ and is modeled as $H_{r,k} = h_r{}^T\,\Phi_r\ g_{r,k}$. Here, $\Phi_r = diag(e^{j\phi_{r,1}}, e^{j\phi_{r,2}}, ..., e^{j\phi_{r,N}})$, where $\phi_{r,n} \in [0, 2\pi)$ denotes the phase shift applied by the nth reflecting element in RIS r. It is assumed that the RIS phase shifts are configured to eliminate the channel phases, thereby maximizing the received SNR at the user end, a common assumption for deriving performance bounds. We consider that the RIS elements exhibit spatial correlation. Let $\mathbf{R}$ denote the correlation matrix, where the (i,j)-th entry is given by $R_{ij} = \rho^{|i-j|}$, with $\rho \in [0,1]$ representing the correlation coefficient [29]. This model implies that the correlation between elements i and j decays exponentially with their physical separation $|i-j|$. It is important to note that $\mathbf{R}$ is symmetric, i.e., $R_{ij} = R_{ji}$, and each diagonal element satisfies $R_{ii} = 1$.

The amplitude of the channel between the BS and element n of RIS r, and that between element n and user k, are respectively given as follows

$$\begin{aligned} |h_{r,n}| &= \acute{r}_r^{-\delta_r/2} \sum_{i=1}^{N} R_{ni}^{1/2}\ \alpha_{r,i} \\ |g^{(k)}_{r,n}| &= (\acute{l}^k_r)^{-\delta_r/2} \sum_{j=1}^{N} R_{nj}^{1/2}\ \beta^{(k)}_{r,j} \end{aligned} \tag{3}$$

where $\acute{r}_r$ and $\acute{l}^k_r$ represent the distances for the links between the BS and RIS r and between the RIS r and user k, respectively, δ_r is the path-loss exponent, and $\alpha_{r,i}$ and $\beta^{(k)}_{r,j}$ are the small-scale fading amplitudes that follow Nakagami-m distribution with shape parameter m_{r_ι} and scale parameter Ω_{r_ι}, with $\iota \in \{1, 2\}$ for the first and second hops, respectively. Thus, the amplitude of the cascaded channel through RIS r can be represented as

$$\begin{aligned} |H_{r,k}| = |h_r|^T\ |g_{r,k}| &= \sum_{n=1}^{N} |h_{r,n}|\ |g^{(k)}_{r,n}| \\ &= \sum_{n=1}^{N} Y^{(k)}_{r,n} \end{aligned} \tag{4}$$

$$Y^{(k)}_{r,n} = \acute{r}_r^{-\delta_r/2}\ (\acute{l}^k_r)^{-\delta_r/2} \sum_{i=1}^{N}\sum_{j=1}^{N} \alpha_{r,i}\ \beta^{(k)}_{r,j}\ R_{ni}^{1/2} R_{nj}^{1/2} \tag{5}$$

III. DELAY ANALYSIS AND LINK SELECTION

This section outlines the average packet delay for successful transmissions over the direct and RIS-assisted links. The delay analysis relies on the underlying channel conditions, the SNR distribution across each available link, and the spatial correlation among RIS elements.

A. CHANNEL ANALYSIS UNDER SPATIAL CORRELATION

For the direct link, the squared channel amplitude $\varkappa_k^2$ follows a Gamma distribution, whose cumulative distribution function (CDF) is given by

$$F_{\varkappa_k^2}(x) = \frac{\gamma(m_{d_k}, \frac{m_{d_k} x}{\Omega_{d_k}})}{\Gamma(m_{d_k})} \tag{6}$$

where $\gamma(.,.)$ is the lower incomplete Gamma function. Then, the received SNR by user k through the direct link can be expressed as

$$\gamma_k = \frac{P|D_k|^2}{N_0} = \overline{\gamma}\ |D_k|^2 \tag{7}$$

where $\overline{\gamma} = P/N_0$, with P denoting the downlink transmit power of the BS and N_0 representing the variance of the additive white Gaussian noise (AWGN) at the user receiver. Thus, the average received SNR at user k via the direct link with the BS is given by

$$\begin{aligned} \mathbb{E}[\gamma_k] &= \overline{\gamma}\ \mathbb{E}[|D_k|^2] \\ &= \overline{\gamma}\ d_k^{-\delta_k}\ \Omega_{d_k} \end{aligned} \tag{8}$$

This article has been accepted for publication in IEEE Access. This is the author's version which has not been fully edited and content may change prior to final publication. Citation information: DOI 10.1109/ACCESS.2025.3626553

For RIS-assisted links, and based on (5), the cascaded channel includes N^2 summation terms that are correlated due to the spatial correlation among RIS elements. To maintain analytical tractability, the spatial correlation in the effective cascaded channel is primarily attributed to the inter-element correlation within the RIS structure, resulting from sub-wavelength spacing and mutual coupling, rather than a direct dependency between $\alpha_{r,i}$ and $\beta_{r,j}^{(k)}$.

We remark that under the exponential correlation model, the spatial correlation between RIS elements is strong when the indices i and j are close, and weakens as the distance $|i-j|$ increases due to the exponential correlation decay. This short-range dependence is generally weak enough for the central limit theorem (CLT) to apply, as long as the covariances do not dominate the total variance. Specifically, when the number of RIS elements N is large, the number of correlated contributions per element becomes sufficiently large, which justifies the CLT under weak dependence [30]. Consequently, the probability density function (PDF) of $Y_{r,n}^{(k)}$ approaches the Gaussian distribution with a mean of $\mu_{Y_{r,n}^{(k)}} = \mathbb{E}[Y_{r,n}^{(k)}]$ and variance of $\sigma^2_{Y_{r,n}^{(k)}}$, i.e., $Y_{r,n}^{(k)} \sim \mathcal{N}(\mu_{Y_{r,n}^{(k)}}, \sigma^2_{Y_{r,n}^{(k)}})$.

The first and second moments of the effective cascaded channel gain $Y_{r,n}^{(k)}$, through element n of RIS r, can be expressed as

$$\begin{aligned}\mathbb{E}[Y_{r,n}^{(k)}] =\ & \acute{r}_r^{-\delta_r/2}\,(\acute{l}_r^k)^{-\delta_r/2}\Big(\prod_{\iota=1}^{2}\frac{\Gamma(m_{r_\iota}+1/2)}{\Gamma(m_{r_\iota})}(\frac{\Omega_{r_\iota}}{m_{r_\iota}})^{1/2}\Big)\\ & *\sum_{i=1}^{N}\sum_{j=1}^{N} R_{ni}^{1/2}R_{nj}^{1/2}\\ \mathbb{E}[(Y_{r,n}^{(k)})^2] =\ & \acute{r}_r^{-\delta_r}(\acute{l}_r^k)^{-\delta_r}\sum_{i=1}^{N}\sum_{j=1}^{N}\sum_{v=1}^{N}\sum_{l=1}^{N}(\mu^2_{\alpha_r}+R_{iv}(\Omega_{r_1}-\mu^2_{\alpha_r}))\\ & *(\mu^2_{\beta_r^{(k)}}+R_{jl}(\Omega^k_{r_2}-\mu^2_{\beta_r^{(k)}}))\,R_{ni}^{1/2}R_{nj}^{1/2}R_{nv}^{1/2}R_{nl}^{1/2}\end{aligned} \tag{9}$$

where $\mathbb{E}[Y_{r,n}^{(k)}]$ is obtained by evaluating the expectation of a double Nakagami-m RV [28], i.e., the product of $\alpha_{r,i}$ and $\beta_{r,j}^{(k)}$. To compute $\mathbb{E}[(Y_{r,n}^{(k)})^2]$, the expectations $\mathbb{E}[\alpha_{r,i}\alpha_{r,v}]$ and $\mathbb{E}[\beta_{r,j}^{(k)}\beta_{r,l}^{(k)}]$ are derived using the definition of covariance, i.e., $Cov(\alpha_{r,i},\alpha_{r,v})$ and $Cov(\beta_{r,j}^{(k)},\beta_{r,l}^{(k)})$, along with the standard expression for the correlation coefficient between elements i and v, and j and l, respectively. The RVs $\alpha_{r,i}$, $\alpha_{r,v}$ (similarly $\beta_{r,j}^{(k)}$, $\beta_{r,l}^{(k)}$) are identically distributed Nakagami-m variables, sharing the same first and second moments, denoted by μ_{α_r} and $\mathbb{E}[\alpha_r^2] = \Omega_{r_1}$ (and $\mu_{\beta_r^{(k)}}$, $\mathbb{E}[(\beta_r^{(k)})^2] = \Omega_{r_2}^{(k)}$). Then, using (9), the variance of $Y_{r,n}^{(k)}$ can be calculated as $\sigma^2_{Y_{r,n}^{(k)}} = \mathbb{E}[(Y_{r,n}^{(k)})^2] - (\mathbb{E}[Y_{r,n}^{(k)}])^2$.

Since $Y_{r,n}^{(k)}$ is approximated by a normal distribution, the sum $\sum_{n=1}^{N} Y_{r,n}^{(k)}$ can also be modeled as a normally distributed RV. However, the resulting distribution reflects a different level of correlation across the cascaded channel components through RIS r. Therefore,

$$\begin{aligned}|H_{r,k}| &= \sum_{n=1}^{N} Y_{r,n}^{(k)} \sim \mathcal{N}(\mu_{|H_{r,k}|}, \sigma^2_{|H_{r,k}|})\\ \mu_{|H_{r,k}|} &= \sum_{n=1}^{N}\mu_{Y_{r,n}^{(k)}}\\ \sigma^2_{|H_{r,k}|} &= \sum_{n=1}^{N}\sigma^2_{Y_{r,n}^{(k)}} + 2\sum_{n<m} Cov(Y_{r,n}^{(k)}, Y_{r,m}^{(k)})\end{aligned} \tag{10}$$

where $Cov(Y_{r,n}^{(k)}, Y_{r,m}^{(k)}) = \mathbb{E}[Y_{r,n}^{(k)}Y_{r,m}^{(k)}] - \mathbb{E}[Y_{r,n}^{(k)}]\mathbb{E}[Y_{r,m}^{(k)}]$, and this expectation can be calculated as follows

$$\begin{aligned}\mathbb{E}[Y_{r,n}^{(k)}Y_{r,m}^{(k)}] &= \acute{r}_r^{-\delta_r}(\acute{l}_r^k)^{-\delta_r}\sum_{i=1}^{N}\sum_{j=1}^{N}\sum_{v=1}^{N}\sum_{l=1}^{N} R_{ni}^{1/2}R_{nj}^{1/2}R_{mv}^{1/2}R_{ml}^{1/2}\\ &\quad *\,\mathbb{E}[\alpha_{r,i}\alpha_{r,v}]\ \mathbb{E}[\beta_{r,j}^{(k)}\beta_{r,l}^{(k)}]\\ &= \acute{r}_r^{-\delta_r}(\acute{l}_r^k)^{-\delta_r}\sum_{i=1}^{N}\sum_{j=1}^{N}\sum_{v=1}^{N}\sum_{l=1}^{N} R_{ni}^{1/2}R_{nj}^{1/2}R_{mv}^{1/2}R_{ml}^{1/2}\\ &\quad *(\mu^2_{\alpha_r}+R_{iv}(\Omega_{r_1}-\mu^2_{\alpha_r}))(\mu^2_{\beta_r^{(k)}}+R_{jl}(\Omega^{(k)}_{r_2}-\mu^2_{\beta_r^{(k)}}))\end{aligned} \tag{11}$$

As $|H_{r,k}|$ is a Gaussian distributed RV with mean $\mu_{|H_{r,k}|}$ and variance $\sigma^2_{|H_{r,k}|}$, the squared magnitude $|H_{r,k}|^2$ follows a non-central chi-square distribution with one degree of freedom. Consequently, the expected value of the channel gain through RIS r is given by

$$\begin{aligned}\mathbb{E}[|H_{r,k}|^2] &= \mu^2_{|H_{r,k}|} + \sigma^2_{|H_{r,k}|}\\ &= (\sum_{n=1}^{N}\mu_{Y_{r,n}^{(k)}})^2 + \Big(\sum_{n=1}^{N}\sigma^2_{Y_{r,n}^{(k)}} + 2\sum_{n<m} Cov(Y_{r,n}^{(k)}, Y_{r,m}^{(k)})\Big)\end{aligned} \tag{12}$$

Thus, the expected SNR received by user k through RIS r is given by

$$\mathbb{E}[\gamma_{r,k}] = \frac{P}{N_0}\ \mathbb{E}[|H_{r,k}|^2] = \overline{\gamma}\ \mathbb{E}[|H_{r,k}|^2] \tag{13}$$

Spatial correlation among RIS elements has a significant impact on the link performance and the expected received SNR. In particular, higher levels of correlation concentrate the channel energy into a dominant eigenmode. By configuring the RIS to align its phase shifts with this dominant eigenmode, the reflected signals can be coherently combined at the intended receiver, thereby enhancing the effective SNR. This effect is particularly pronounced in scenarios where the RIS serves a single user or a single data stream, as the constructive combination of signals in the dominant mode maximizes the achievable array gain. As a special case, consider the scenario where the channels experience Rayleigh fading, i.e., $m_{r_1} = m_{r_2} = 1$. In this case, the mean values of the channel amplitudes are given by

$$\mu_{\alpha_r} = \frac{\sqrt{\pi\ \Omega_{r_1}}}{2}, \qquad \mu_{\beta_r^{(k)}} = \frac{\sqrt{\pi\ \Omega_{r_2}^{(k)}}}{2} \tag{14}$$

We examine two limiting cases of spatial correlation among the RIS elements, specifically the fully correlated and uncorrelated cases. In the fully correlated case, $\rho = 1$, which implies $R_{ij} = 1$ for all i, j. Therefore, using (9) and (14), the statistical moments of the cascaded channel through element n in RIS r can be expressed as

$$\begin{aligned}\mathbb{E}[Y_{r,n}^{(k)}] &= \frac{\pi}{4}\, \acute{r}_r^{-\delta_r/2}\, (\acute{l}_r^k)^{-\delta_r/2} \sqrt{\Omega_{r_1}\Omega_{r_2}^{(k)}}\, N^2 \\ \mathbb{E}[(Y_{r,n}^{(k)})^2] &= \acute{r}_r^{-\delta_r} (\acute{l}_r^k)^{-\delta_r}\, N^4\, \Omega_{r_1}\Omega_{r_2}^{(k)}\end{aligned} \tag{15}$$

Using (10), the mean and variance of the overall cascaded channel $|H_{r,k}|$ for the fully correlated case are given by

$$\begin{aligned}\mu_{|H_{r,k}|} &= \frac{\pi}{4}\, \acute{r}_r^{-\delta_r/2}\, (\acute{l}_r^k)^{-\delta_r/2}\, N^3 \sqrt{\Omega_{r_1}\Omega_{r_2}^{(k)}} \\ \sigma^2_{|H_{r,k}|} &= \acute{r}_r^{-\delta_r} (\acute{l}_r^k)^{-\delta_r}\, N^6\, \Omega_{r_1}\Omega_{r_2}^{(k)}\, (1 - \frac{\pi^2}{16})\end{aligned} \tag{16}$$

Thus, the average received SNR at user k is $\mathbb{E}[\gamma_{r,k}] = \overline{\gamma}\, \acute{r}_r^{-\delta_r} (\acute{l}_r^k)^{-\delta_r} \Omega_{r_1}\Omega_{r_2}^{(k)} N^6$.

For uncorrelated elements, the correlation matrix reduces to the identity matrix, i.e., $\mathbf{R} = \mathbf{I}_N$. Consequently, the covariance between channels corresponding to any pair of elements n and m vanishes, i.e., $Cov(Y_{r,n}^{(k)}, Y_{r,m}^{(k)}) = 0$, since the expectation values satisfy $\mathbb{E}[Y_{r,n}^{(k)} Y_{r,m}^{(k)}] = \mathbb{E}[Y_{r,n}^{(k)}]^2 = \frac{\pi^2}{16}\, \acute{r}_r^{-\delta_r} (\acute{l}_r^k)^{-\delta_r} \Omega_{r_1}\Omega_{r_2}^{(k)}$. Accordingly, the expected SNR received by user k through RIS r with uncorrelated elements is given by $\mathbb{E}[\gamma_{r,k}] = \overline{\gamma}\, \acute{r}_r^{-\delta_r} (\acute{l}_r^k)^{-\delta_r} \Omega_{r_1}\Omega_{r_2}^{(k)}\, N \left(\frac{\pi^2}{16}(N-1)+1\right)$.

It is evident that when all RIS elements are fully correlated, the SNR scales as N^6, whereas in the uncorrelated case, it scales only as N^2 when the entire RIS is used to serve one user. This difference illustrates that, by optimizing the RIS phases to align with the intended user, a strong spatial correlation can significantly enhance the constructive combination of reflected signals. These findings underscore the importance of incorporating spatial correlation in RIS design and optimization to fully leverage the potential of intelligent reflections in wireless communication systems.

B. PACKET DELAY AND LINK SELECTION

The objective is to minimize the network's average packet delay, a key metric for supporting delay-sensitive applications. Therefore, selecting the most appropriate link for each user is essential for efficient communication. Depending on user location, available links may include direct and RIS-assisted paths, with some users limited to direct links and others relying on RIS connections. For instance, as illustrated in Fig. 1, user 1 has four feasible links: the direct link and RIS-assisted links via RIS 2, RIS 3, and RIS 4.

Building on the previous analysis, the received SNR γ_k of the direct BS-user k link under Nakagami-m fading follows a Gamma distribution, whose CDF is expressed as

$$F_{\gamma_k}(\theta) = \frac{\gamma(m_{d_k}, \frac{m_{d_k}}{\Omega_{d_k}} \frac{\theta d_k^{\delta_k}}{\overline{\gamma}})}{\Gamma(m_{d_k})} \tag{17}$$

For the RIS r-assisted link, the CDF of $\gamma_{r,k}$ can be given as follows

$$F_{\gamma_{r,k}}(\theta) = 1 - Q_{\frac{1}{2}}(\frac{\sqrt{\lambda_{r,k}}}{\sigma_{|H_{r,k}|}}, \frac{\sqrt{\theta}}{\sqrt{\overline{\gamma}}\, \sigma_{|H_{r,k}|}}) \tag{18}$$

where Q_ς(a,b) is the Marcum Q-function and defined in [31], and $\lambda_{r,k} = \mu^2_{|H_{r,k}|}$.

The delay analysis employs an adaptive M-QAM modulation scheme, where the modulation order is dynamically adjusted according to the channel conditions. To evaluate the average transmission delay of a packet, the SNR range is partitioned into $\grave{L}$ distinct regions, each associated with a specific modulation level determined by the underlying SNR distribution. In region ν, a modulation scheme with constellation size $M_\nu = 2^\nu$ is employed, where ν= 1,2,3,..., $\grave{L}$. For the adaptive discrete-rate strategy, the SNR switching thresholds are determined based on a target bit error rate (BER_{th}), and given by [32]

$$\theta_\nu = \begin{cases} [erfc^{-1}(2BER_{th})]^2, & \nu = 1. \\ \frac{2}{3}K_0(2^\nu - 1), & \nu = 2, 3, ..., \grave{L}. \end{cases} \tag{19}$$

where $erfc^{-1}()$ is the inverse complementary error function, and $K_0 = -\ln(5BER_{th})$.

The average link data rate of the adaptive M-QAM scheme with discrete rate is the sum of the data rates ($log_2[M_\nu] = \nu$) associated with the individual $\grave{L}+1$ regions, weighted by the probability $a_\nu = \int_{\theta_\nu}^{\theta_{\nu+1}} p_\gamma(\gamma)d\gamma$ that the SNR γ falls in the ν-th region [33]. Therefore, the average data rate for the user k can be expressed as

$$\begin{aligned}R_k &= B_k \sum_{\nu=1}^{\grave{L}} \left(log_2[M_\nu].\int_{\theta_\nu}^{\theta_{\nu+1}} p_\gamma(\gamma)d\gamma\right) \\ &= B_k \sum_{\nu=1}^{\grave{L}} \nu.\, a_\nu\end{aligned} \tag{20}$$

where B_k denotes the bandwidth allocated to user k. The probability a_ν is given by

$$a_\nu = \int_{\theta_\nu}^{\theta_{\nu+1}} p_\gamma(\gamma)d\gamma = F_\gamma(\theta_{\nu+1}) - F_\gamma(\theta_\nu) \tag{21}$$

where γ represents either γ_k or $\gamma_{r,k}$, corresponding to the direct and RIS-assisted links, respectively. For each feasible link, whether direct or RIS-assisted link, the probability a_ν for all SNR regions is determined based on (17) and (18). Subsequently, the average packet delay, D_k, for transmitting a packet of size Q bits, is calculated as the packet size Q (in bits) divided by the average data rate R_k (in bits/second) in equation (20), that can be expressed as $D_k = Q/R_k$.

To select the optimal transmission path for each user, we adopt a delay-aware link-selection strategy that jointly considers the expected received SNR and the resulting packet delay. The direct link between user k and BS outperforms the RIS-assisted link r when it provides a higher expected received SNR, i.e. when $\mathbb{E}[\gamma_k] > \mathbb{E}[\gamma_{r,k}]$. Using (8) and (13), the

This article has been accepted for publication in IEEE Access. This is the author's version which has not been fully edited and
content may change prior to final publication. Citation information: DOI 10.1109/ACCESS.2025.3626553

distance condition under which the direct link outperforms the RIS-assisted link r can be expressed as

$$d_k < \left[\frac{\Omega_{d_k}}{(\sum_{n=1}^{N} \mu_{Y_{r,n}})^2 + \sum_{n=1}^{N} \sigma^2_{Y_{r,n}} + 2\sum_{n<m} \mathrm{Cov}(Y_{r,n}, Y_{r,m})} \right]^{1/\delta_k} \tag{22}$$

This condition serves as a criterion to determine whether an RIS link can provide a higher SNR than the direct link. An RIS r is considered a feasible option for user k only if this condition is not satisfied.

For a given user k, the expected SNR is first evaluated over all feasible paths, including the direct link and RIS-assisted links, while explicitly accounting for the spatial correlation among RIS elements. For each candidate path, the expected packet delay is computed by incorporating both the statistical characterization of the cascaded channels and the effects of spatial correlation, providing an accurate estimate of the effective service time per path. The path that minimizes the expected packet delay is then selected as the preferred transmission link. This approach ensures that the chosen path maintains high link quality while directly targeting latency reduction. Notably, neglecting the spatial correlation among RIS elements may result in suboptimal link selection, which can degrade system delay performance. For example, ignoring the correlation among RIS elements during the selection process can result in an RIS-assisted link being incorrectly perceived as incurring a higher delay than the direct link, leading to its exclusion, even though it may in fact offer superior delay performance. Finally, after determining the optimal path for each user, the average delay across all users is calculated to assess the overall network performance.

IV. PERFORMANCE EVALUATION

In this section, we investigate the impact of spatial correlation among RIS elements on delay performance and its influence on link selection and user association. Packet delay depends on factors such as average transmit SNR, the number of RIS elements, and transmission distances. We also analyze system performance and RIS selection under different fading conditions. To validate the derived analytical expressions, we conduct Monte Carlo (MC) simulations. A large number of channel realizations are generated using Nakagami-m fading for all feasible links of each user. The direct and cascaded RIS-assisted channels are then obtained, and the SNR performance is evaluated without relying on assumptions made in the analytical derivation, such as the CLT.

The BS is placed at the origin (0,0) and assisted by $I = 5$ RISs to support K randomly distributed users. Unless stated otherwise, system parameters include a 100 MHz downlink bandwidth, a path loss exponent of 2.2, $\rho = 0.5$, and a packet size of 1500 bytes. The Nakagami-m fading parameters m_{d_k} and m_{r_ι} are selected from the set $[0.5, 1, 2, 3]$, based on fading severity, while the scale parameter Ω is set to 2. We divide the SNR range into six regions, $\grave{L} = 6$, each assigned a modulation order based on predefined boundaries targeting a BER of 10^{-5}.

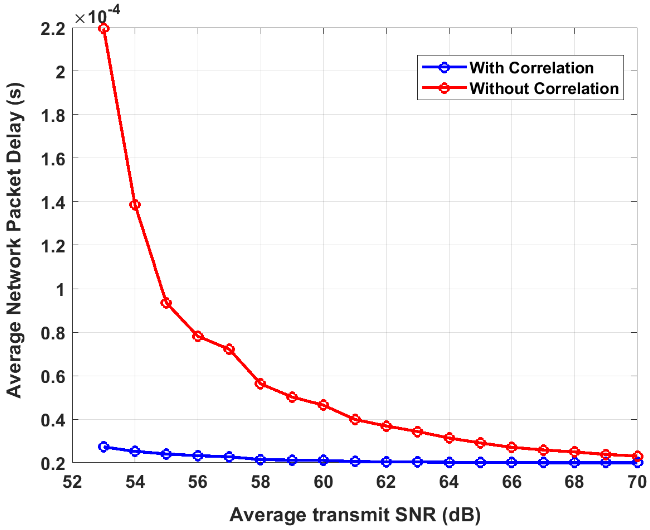

FIGURE 2. Average network packet delay versus average transmit SNR for systems with and without RIS element correlation, when $\rho = 0.5$.

We compare our delay-aware selection approach against two benchmarks: random selection among feasible links and shortest path selection, which represent naive and distance-based approaches, respectively.

Fig. 2 illustrates the average network packet delay versus the average transmit SNR $\overline{\gamma}$ for systems with and without considering RIS elements correlation. In the considered setup, users are randomly distributed, and for each user, a set of feasible links is determined based on the distance condition in (22), which specifies whether the direct BS link outperforms a given RIS-assisted link. The link exhibiting the highest received SNR is then selected to maximize the data rate and minimize the transmission delay. The results demonstrate the importance of considering RIS elements correlation in delay analysis, as neglecting it leads to inaccurate packet delay estimations and suboptimal link selections that significantly degrade performance. As observed in Fig. 2, incorporating RIS correlation substantially improves the delay performance across all transmit SNR values. This is because a higher correlation concentrates channel energy into a dominant eigenmode when serving a single user at a time, with RIS phase shifts configured to coherently combine the N reflected signals at the receiver. In contrast, ignoring correlation results in fewer coherent combining, lower received SNR, and increased packet delay.

In Fig. 3, the average packet delay is shown as a function of the average transmit SNR for different correlation levels of RIS elements. The results show that a higher correlation significantly improves the delay performance. When $\rho = 1$, the delay remains nearly constant at a low value across the SNR range, indicating efficient coherent combining of the reflected signals. As the correlation decreases, particularly at $\rho = 0.5$, the delay increases notably and becomes more sensitive to the changes in transmit SNR. This behavior

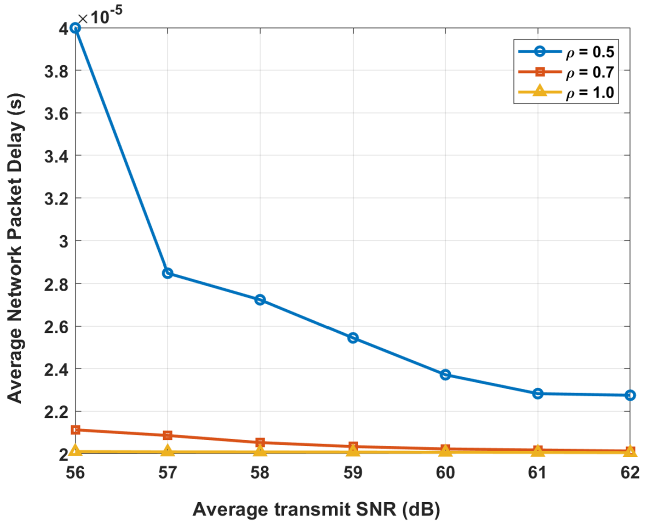

FIGURE 3. The relationship of average packet delay and average transmit SNR for different correlation levels of RIS elements.

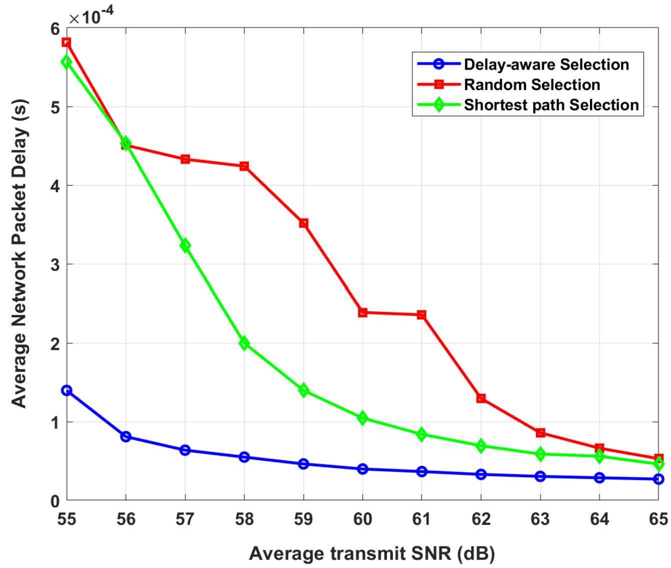

FIGURE 4. Average packet delay versus transmit SNR for different link selection strategies, when $\rho = 0.5$.

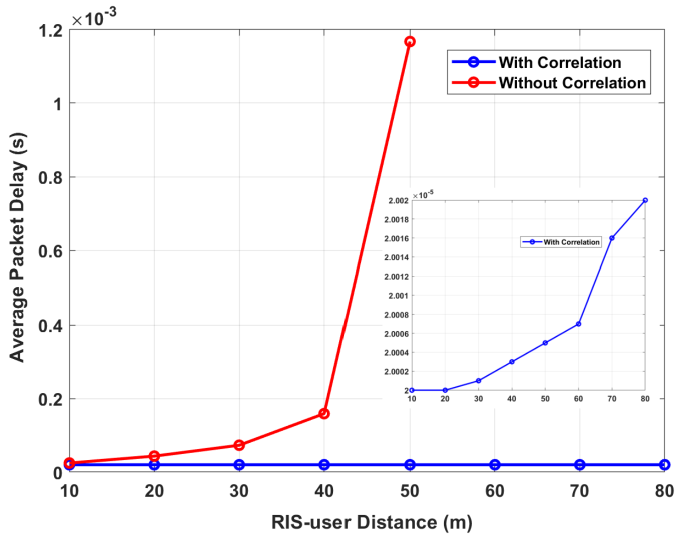

FIGURE 5. Average packet delay versus RIS-user distance with and without considering RIS element correlation.

demonstrates that a stronger correlation enhances the RIS energy focusing capability, resulting in better effective received SNR and reduced packet delays. Fig. 4 illustrates the average network packet delay as a function of the average transmit SNR for three different link selection strategies: delay-aware selection, shortest path selection, and random selection. In the delay-aware path selection, the link with the highest expected SNR and lowest delay is selected to optimize network performance. In contrast, shortest path selection chooses the closest link, ignoring channel conditions and delay, while random selection assigns a link randomly from the available direct and RIS-assisted options. The results demonstrate that the delay-aware approach consistently achieves the lowest packet delays across all SNR values, highlighting the effectiveness of incorporating SNR and delay expectations into the link selection process. For example, at a transmit SNR of 55dB, the delay-aware selection reduces packet delay by approximately 75% compared to both the random and shortest path approaches. Although the shortest path selection outperforms the random approach, it still yields higher delays compared to the delay-aware method, as it neglects channel conditions and may select suboptimal links in terms of SNR. Random selection results in the worst delay performance, reflecting the inefficiency of random link decisions.

In Fig. 5, the average packet delay is shown as a function of RIS-user distance for a selected user, comparing the cases with and without considering the correlation of RIS elements. When the correlation is considered in the analysis, a slight increase in the packet delay is observed with distance, as shown in the inset plot, where the values range from approximately 2×10^{-5} to 2.002×10^{-5} seconds. Therefore, by capturing the correlation effects, the system can sustain lower delays over longer RIS-user distances, whereas ignoring correlation leads to rapid delay degradation as the distance increases. Fig. 6 shows the average packet delay versus the correlation coefficient ρ for different transmit SNR values. The results show that higher correlation leads to lower packet delays, with the effect being more pronounced at lower SNR values. As ρ increases, the delay rapidly decreases, reflecting the improvement in effective SNR. These results highlight the importance of optimizing RIS fabrication and properly accounting for the spatial correlation between RIS elements, as neglecting it can significantly impact the delay performance. Therefore, correlation should be carefully considered during system analysis, link selection, and RIS association processes.

Fig. 7 illustrates the impact of RIS element correlation on the average network data rate during the selection process. The selection criterion jointly considers both the expected

This article has been accepted for publication in IEEE Access. This is the author's version which has not been fully edited and content may change prior to final publication. Citation information: DOI 10.1109/ACCESS.2025.3626553

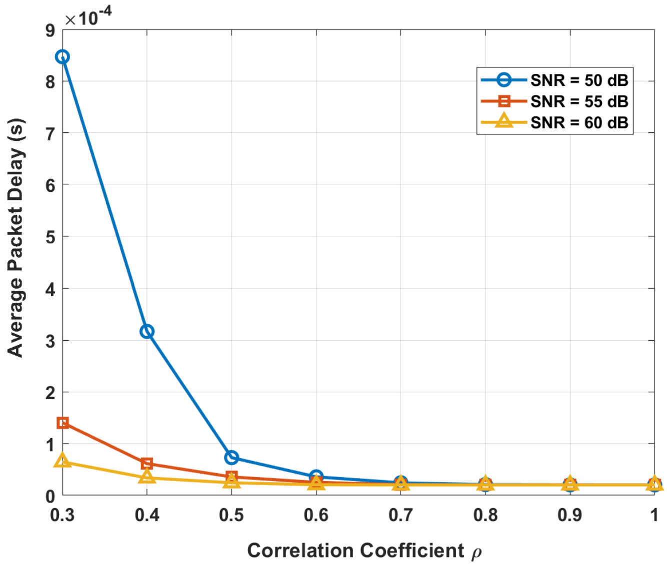

FIGURE 6. Average packet delay variation with the correlation coefficient for different transmit SNR values.

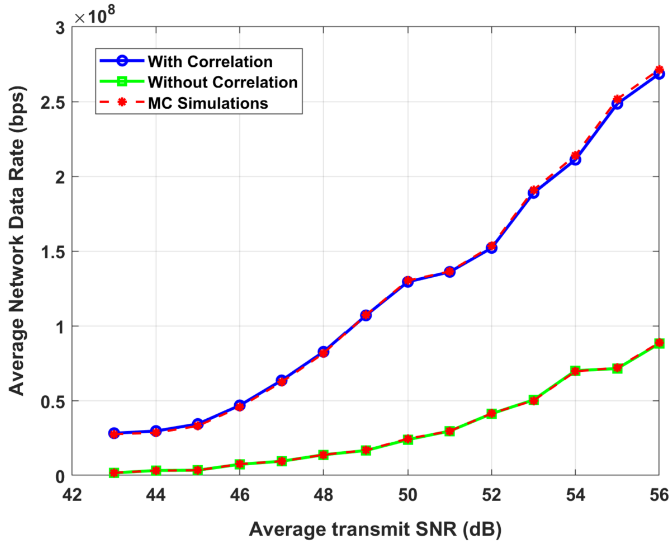

FIGURE 7. Average network data rate versus transmit SNR, with and without RIS element correlation, for $\rho = 0.5$.

received SNR and the associated delay, ensuring that each user is assigned the most reliable transmission path. It can be observed that accounting for RIS element correlation results in a significantly higher network data rate across the entire SNR range. This improvement arises because the correlation among RIS elements influences the effective channel gains, and incorporating it in the selection process avoids inaccurate assessments of link quality. In contrast, ignoring RIS correlation often leads to the selection of suboptimal links, causing a substantial reduction in overall network performance.

Furthermore, the analytical and MC simulation results exhibit strong agreement in both scenarios– considering correlation and ignoring it, thereby confirming the validity of the proposed analytical expressions. Overall, the results highlight that accurate modeling of RIS element correlation is crucial for link selection strategies, as overlooking it can lead to erroneous decisions that severely compromise the achievable data rate and delay performance of the network.

V. CONCLUSION

This paper studies link selection and RIS-user association in multi-RIS networks to minimize average packet delay. We analyze the effect of spatial correlation among RIS elements on the SNR distribution and derive a closed-form condition to identify when the direct link outperforms RIS-assisted links. The average packet delay is then evaluated considering adaptive M-QAM modulation. Results show that accounting for RIS correlation significantly improves delay performance, while neglecting it leads to suboptimal selections. Although correlation is not actively controlled, considering its effect enables more accurate delay assessment and more reliable link selection. In particular, strong spatial correlation concentrates channel energy into a dominant eigenmode for single-user transmission, thereby improving average data rate and delay performance. The delay-aware selection introduced in this work achieves a significantly lower average delay than random and shortest-path methods. In future work. we will explore the impact of spatial correlation in large RIS deployments, where elements are partitioned to serve multiple users simultaneously. We will also explore channel rank or degrees of freedom metrics, investigate imperfect channel estimation and alternative correlation models to further optimize RIS-assisted systems.

REFERENCES

[1] N. Sharma, S. Gautam, A. Kaushik, S. Chatzinotas, and B. Ottersten, "Fractional Programming Strategy for Rate-Energy Optimization in RIS-assisted SWIPT IoT Networks," in *IEEE Global Communications Conference*, 2024, pp. 5126–5131.

[2] Y. Cao, S. Xu, J. Liu, and N. Kato, "IRS Backscatter Enhancing Against Jamming and Eavesdropping Attacks," *IEEE Internet of Things Journal*, vol. 10, no. 12, pp. 10 740–10 751, 2023.

[3] S. Gong, X. Lu, D. T. Hoang, D. Niyato, L. Shu, D. I. Kim, and Y.-C. Liang, "Toward Smart Wireless Communications via Intelligent Reflecting Surfaces: A Contemporary Survey," *IEEE Communications Surveys Tutorials*, vol. 22, no. 4, pp. 2283–2314, 2020.

[4] X. Yu, V. Jamali, D. Xu, D. W. K. Ng, and R. Schober, "Smart and Reconfigurable Wireless Communications: From IRS Modeling to Algorithm Design," *IEEE Wireless Communications*, vol. 28, no. 6, pp. 118–125, 2021.

[5] J. Chen, Y. Xie, X. Mu, J. Jia, Y. Liu, and X. Wang, "Energy Efficient Resource Allocation for IRS Assisted CoMP Systems," *IEEE Transactions on Wireless Communications*, vol. 21, no. 7, pp. 5688–5702, 2022.

[6] Y. Bian, D. Dong, J. Jiang, and K. Song, "Performance Analysis of Reconfigurable Intelligent Surface-Assisted Wireless Communication Systems Under Co-Channel Interference," *IEEE Open Journal of the Communications Society*, vol. 4, pp. 596–605, 2023.

[7] Y. Cao, T. Lv, and W. Ni, "Intelligent Reflecting Surface Aided Multi-User mmWave Communications for Coverage Enhancement," in *IEEE 31st Annual International Symposium on Personal, Indoor and Mobile Radio Communications*, 2020, pp. 1–6.

[8] D. Zhao, H. Lu, Y. Wang, H. Sun, and Y. Gui, "Joint Power Allocation and User Association Optimization for IRS-Assisted mmWave Systems," *IEEE Transactions on Wireless Communications*, vol. 21, no. 1, pp. 577–590, 2022.

[9] Z. Yang, M. Chen, W. Saad, W. Xu, M. Shikh-Bahaei, H. V. Poor, and S. Cui, "Energy-Efficient Wireless Communications With Distributed Reconfigurable Intelligent Surfaces," *IEEE Transactions on Wireless Communications*, vol. 21, no. 1, pp. 665–679, 2022.

[10] R. Hindustani, D. Dixit, S. Sharma, and V. Bhatia, "Outage Probability of Multiple-IRS-Assisted SISO Wireless Communications over Rician Fading," *Physical Communication*, vol. 59, p. 102102, 2023.

[11] Z. Zhang, Y. Cui, F. Yang, and L. Ding, "Analysis and Optimization of Outage Probability in Multi-Intelligent Reflecting Surface-Assisted Systems," *arXiv preprint arXiv:1909.02193*, 2019.

[12] B. C. Nguyen, T. M. Hoang, N. Van Vinh, G. T. Luu *et al.*, "On Performance of Multi-RIS Assisted Multi-User Nonorthogonal Multiple Access System over Nakagami-m Fading Channels," *Computer Communications*, vol. 197, pp. 294–305, 2023.

[13] C. Psomas, H. A. Suraweera, and I. Krikidis, "On the Association with Intelligent Reflecting Surfaces in Spatially Random Networks," in *ICC 2021 - IEEE International Conference on Communications*, 2021, pp. 1–6.

[14] J. Lyu and R. Zhang, "Hybrid Active/Passive Wireless Network Aided by Intelligent Reflecting Surface: System Modeling and Performance Analysis," *IEEE Transactions on Wireless Communications*, vol. 20, no. 11, pp. 7196–7212, 2021.

[15] M. Jung, W. Saad, M. Debbah, and C. S. Hong, "Asymptotic Optimality of Reconfigurable Intelligent Surfaces: Passive Beamforming and Achievable Rate," in *ICC 2020 - IEEE International Conference on Communications (ICC)*, 2020, pp. 1–6.

[16] W. Mei and R. Zhang, "Performance Analysis and User Association Optimization for Wireless Network Aided by Multiple Intelligent Reflecting Surfaces," *IEEE Transactions on Communications*, vol. 69, no. 9, pp. 6296–6312, 2021.

[17] Q. Bie, Z. Liang, Y. Liu, Q. Wu, X. Zhao, and X. Y. Zhang, "User Association for Reconfigurable Intelligent Surfaces Aided Cell-Free Networks," *IEEE Transactions on Vehicular Technology*, vol. 72, no. 11, pp. 14 456–14 467, 2023.

[18] J. Mirza, B. Ali, and M. A. Javed, "Stable Matching for Selection of Intelligent Reflecting Surfaces in Multiuser MISO Systems," *IEEE Communications Letters*, vol. 25, no. 8, pp. 2748–2752, 2021.

[19] Q. Sun, Y. Wu, X. Chen, and J. Zhang, "SLNR-Based Joint RIS-UE Association and Beamforming Design for Multi-RIS Aided Wireless Communications," *IEEE Transactions on Vehicular Technology*, vol. 73, no. 6, pp. 8660–8670, 2024.

[20] C. Chen, F. Wu, C. Zhang, D. Cheng, W. Fan, and Y. Liu, "Joint Optimization of RIS-User Association and Beamforming Design for Multi-RIS-Assisted Multi-User Systems," *IEEE Wireless Communications Letters*, pp. 1–1, 2025.

[21] G. S. Chandra, R. K. Singh, S. Dhok, P. K. Sharma, and P. Kumar, "Downlink URLLC System Over Spatially Correlated RIS Channels and Electromagnetic Interference," *IEEE Wireless Communications Letters*, vol. 11, no. 9, pp. 1950–1954, 2022.

[22] V. Shahiri, H. Behroozi, A. Kuhestani, and K.-K. Wong, "Reconfigurable-Intelligent-Surface-Assisted Secret Key Generation Under Spatially Correlated Channels in Quasi-Static Environments," *IEEE Internet of Things Journal*, vol. 11, no. 9, pp. 15 808–15 822, 2024.

[23] Q. Peng, H. Ren, C. Pan, M. Elkashlan, A. García Armada, and P. Popovski, "Two-Timescale Design for Reconfigurable Intelligent Surface-Aided URLLC," *IEEE Transactions on Wireless Communications*, vol. 23, no. 10, pp. 13 664–13 677, 2024.

[24] M.-M. Zhao, Q. Wu, M.-J. Zhao, and R. Zhang, "Intelligent Reflecting Surface Enhanced Wireless Networks: Two-Timescale Beamforming Optimization," *IEEE Transactions on Wireless Communications*, vol. 20, no. 1, pp. 2–17, 2021.

[25] T. Van Chien, A. K. Papazafeiropoulos, L. T. Tu, R. Chopra, S. Chatzinotas, and B. Ottersten, "Outage Probability Analysis of IRS-Assisted Systems Under Spatially Correlated Channels," *IEEE Wireless Communications Letters*, vol. 10, no. 8, pp. 1815–1819, 2021.

[26] E. Björnson and L. Sanguinetti, "Rayleigh Fading Modeling and Channel Hardening for Reconfigurable Intelligent Surfaces," *IEEE Wireless Communications Letters*, vol. 10, no. 4, pp. 830–834, 2021.

[27] B. Zheng, C. You, and R. Zhang, "Double-IRS Assisted Multi-User MIMO: Cooperative Passive Beamforming Design," *IEEE Transactions on Wireless Communications*, vol. 20, no. 7, pp. 4513–4526, 2021.

[28] G. K. Karagiannidis, N. C. Sagias, and P. T. Mathiopoulos, "$N*$Nakagami: A Novel Stochastic Model for Cascaded Fading Channels," *IEEE Transactions on Communications*, vol. 55, no. 8, pp. 1453–1458, 2007.

[29] R. K. Mallik, "The Exponential Correlation Matrix: Eigen-Analysis and Applications," *IEEE Transactions on Wireless Communications*, vol. 17, no. 7, pp. 4690–4705, 2018.

[30] E. L. Lehmann, *Elements of Large-Sample Theory*. Springer, 1999.

[31] V. M. Kapinas, S. K. Mihos, and G. K. Karagiannidis, "On the Monotonicity of the Generalized Marcum and Nuttall Q -Functions," *IEEE Trans. on Inf. Theory*, vol. 55, no. 8, pp. 3701–3710, 2009.

[32] A. I. Abdulshakoor, N. A. Ali, and H. S. Hassanein, "A Comprehensive Analysis of Packet Delay in Reconfigurable Intelligent Surface-Assisted Communication Networks," in *ICC 2024 - IEEE International Conference on Communications*, 2024, pp. 1691–1696.

[33] M.-S. Alouini and A. J. Goldsmith, "Adaptive modulation over Nakagami fading channels," *Wireless Personal Communications*, vol. 13, pp. 119–143, 2000.

AHMED I. ABDULSHAKOOR received the B.S. (Hons.) and M.S. degrees in electronics and electrical communications engineering from Menoufia University, Menouf, Egypt, in 2015 and 2020, respectively. He is currently working toward a Ph.D. degree in electrical and computer engineering at Queen's University, Kingston, Canada. He is on leave from the Faculty of Electronic Engineering, Menoufia University, Egypt. From 2016 to 2019, he was a Research Assistant at the National Telecommunications Regularity Authority, Egypt. His research interests include wireless communications, information theory, and next-generation wireless access networks.

NAJAH ABU ALI received the B.Sc. and M.Sc. degrees in electrical engineering from the University of Jordan and the Ph.D. degree in computer networks from the Department of Electrical and Computer Engineering, Queen's University, Kingston, Canada. She is currently a Professor with the College of Information Technology, United Arab Emirates University (UAEU). Her work has been consistently published in key publications venues-journals and conferences. Her general research interests include modeling wireless communications, resource management in wireless networks. More recently, she has strengthened her focus on the Internet of Things, Vehicle-to-vehicle networking, and 6G sensing. She has also delivered various seminars and tutorials at flagship conferences such as the IEEE Communication Society conferences. She has also served as an organizer, committee chair, and a TPC Member for several flagship conferences, including ICC and GLOBECOM, and contributed to the organization of several special issue journals and workshops.

HOSSAM HASSANEIN (S'85, M'90, SM'05, F'17) is a leading researcher in the areas of broadband, wireless and mobile networks architecture, protocols, control and performance evaluation. His record spans more than 600 publications in journals, conferences and book chapters, in addition to numerous keynotes and Tutorials in flagship venues. Dr. Hassanein has received several recognition and best paper awards at top international conferences. He is the founder and director of the Telecommunications Research Lab (TRL) at Queen's University School of Computing, with extensive international academic and industrial collaborations. He is the recipient of the 2016 IEEE Communications Society Communications Software Technical Achievement Award for outstanding contributions to routing and deployment planning algorithms in wireless sensor networks, and the 2020 IEEE IoT, Ad Hoc and Sensor Networks Technical Achievement and Recognition Award for significant contributions to technological advancement of the Internet of Things, ad hoc networks and sensing systems. Dr. Hassanein is a fellow of the IEEE, and is a former chair of the IEEE Communication Society Technical Committee on Ad hoc and Sensor Networks (TC AHSN). He is an IEEE Communications Society Distinguished Speaker (Distinguished Lecturer 2008-2010).